American Mineralogist, Volume 77, pages 1031–1037, 1992

Possible prograde fluid inclusions in recrystallized chert nodules in a contact aureole, Christmas Mountains, Texas

Sakiko N. Olsen
Department of Earth and Planetary Sciences, The Johns Hopkins University, Baltimore, Maryland 21218, U.S.A.
Lukas P. Baumgartner, Philip E. Brown
Department of Geology and Geophysics, University of Wisconsin, Madison, Wisconsin 53706, U.S.A.

Abstract

Quartz grains in recrystallized chert nodules from contact-metamorphosed limestones of the Christmas Mountains, Texas, contain clusters of fluid inclusions of <1–3 μm, except in a zone near the intrusive contact. At 70 m from the contact, these inclusions form uniform clouds in the cores of the grains, surrounded by narrow inclusion-free rims. At 50 m, the inclusion clouds are found only in some of the grains and occupy <2–3 vol% at the core. Nodules close to the contact (<12 m) have no clouds. The inclusions in the clouds contain mainly CO_2 and H_2O, as determined by microthermometric, Raman, and micro-FTIR analyses. The mode of occurrence suggests that these inclusions were the earliest to form and contain fluids internally generated, most likely by the breakdown of organic matter in chert. This is thought to have occurred before peak metamorphism. The presence of larger inclusions, also containing mainly CO_2-H_2O, on the periphery of some clouds suggests that some small inclusions coalesced into larger ones. This coalescing process may have formed some of the inclusions present in the higher-grade nodules, which appear to be not directly associated with a cloud, although most were probably formed later. Inclusion-free rims in the lower-grade quartz suggest that some of the fluids from early inclusions were freed by dissolution and reprecipitation and by recrystallization of quartz and were lost from the rock. The absence of inclusion clouds at the highest grade is attributed to this loss. The preservation in inclusions of fluids generated during a prograde process (before peak metamorphism) does not necessarily rule out the peak metamorphic influx of fluids. However, stable isotope analyses also indicate the absence of a pervasive flow of external fluids through the nodules during peak metamorphism.

Introduction

Fluid inclusions in metamorphic rocks are generally thought to have trapped a discrete metamorphic fluid phase (Crawford and Hollister, 1986). Experimental studies have shown clearly that it is possible under metamorphic conditions to trap a representative sample of coexisting fluid in inclusions (e.g., Sterner et al., 1988). The inclusions may be primary, trapping fluid present during the growth of the mineral, or secondary, trapping a later fluid in a fracture that traversed a preexisting grain (Roedder, 1984). Another, and generally minor, category consists of pseudosecondary inclusions (Roedder, 1984, p. 23), which trap fluid in a fracture formed in a growing mineral. In metamorphic rocks in general, primary and pseudosecondary inclusions should contain the peak metamorphic fluid. Such fluid is assumed to have been in equilibrium with the observed peak metamorphic mineral assemblage (see Ferry and Burt, 1982). A later fluid, in secondary inclusions, is not likely to have been in equilibrium with the primary mineral assemblage, although it may have equilibrated with the host mineral or a retrograde alteration assemblage. There is yet a fourth category of fluid inclusions that is not often considered. These inclusions contain fluid generated internally in the host. They include exsolution inclusions (Spear and Selverstone, 1983; Roedder, 1984, p. 35) but not all internally generated fluids have to be exsolved from a mineral in the strict sense. The fluid could instead have formed during a prograde process from material originally contained in the ultimate inclusion host. We apply the term "prograde" in this paper to that portion of the *P-T-t* path before peak conditions were attained during which temperatures were increasing. Identification of such prograde inclusions with internally generated fluid has important implications for the interpretation of fluid inclusions in metamorphic rocks. These inclusions may be falsely interpreted as peak metamorphic (primary) inclusions because they would tend to occur as the texturally earliest inclusions (as isolated inclusions in the core of a grain, not in healed fractures). Generally, all inclusions formed during the prograde process are thought to be destroyed by heating, deformation, and recrystallization of the mineral host during peak metamorphism (but see Mullis, 1987, p. 170; Vry and Brown, 1991). Consequently, it

0003–004X/92/0910–1031$02.00

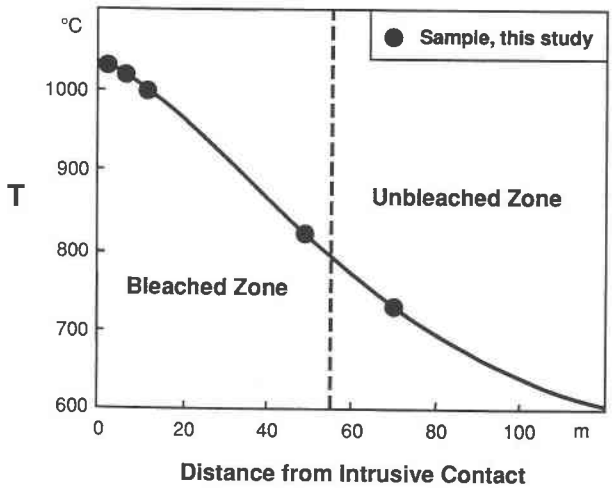

Fig. 1. Maximum temperature profile after Joesten (1983). Dashes: approximate contact between bleached and unbleached zones of aureole.

has been a general practice to expect the earliest inclusions to contain peak metamorphic fluid (but see Hollister, 1990). Such fluid should have a composition consistent with the mineral assemblage, which is calculated using thermochemical data and equations of state (e.g., Ferry and Burt, 1982). The composition of an internally derived fluid, on the other hand, need not agree with the calculated composition because it was probably not in equilibrium with the peak metamorphic mineral assemblage. This could explain some of the puzzling cases where the composition of the texturally earliest fluid inclusion does not agree with calculated fluid. We present in this paper an example of such inclusions found in recrystallized chert nodules in a contact aureole in the Christmas Mountains, Texas. The composition and distribution of these inclusions suggest that the fluids were derived internally from within chert, most likely as the breakdown products of organic matter during a prograde process. These early-formed inclusions were lost from the higher-grade rocks.

Geological setting and previous studies

The lower Cretaceous limestone in the Christmas Mountains was intruded by an early Tertiary composite stock of alkali gabbro and syenite that formed a high-temperature contact aureole. The aureole is divided into an inner bleached marble (marble aureole of Joesten, 1976) and an outer, gray, unbleached zone in which organic matter is present. At the intrusive contact itself the temperature was high enough (~1000 °C, Fig. 1) to form spurrite, with a load pressure estimated at ~325 bars (Joesten, 1983). Some layers of the St. Elena limestone in the Christmas Mountains contain abundant chert nodules, approximately 2–15 by 2–15 by 5–25 cm in size, with the longest axis parallel to the sedimentary layering. Contact metamorphic effects led to the formation of concentric mineral zonations as reaction rims of calc-silicates around these nodules. Joesten (e.g., 1974) and Joesten and Fisher (1988) have successfully modeled the formation of calc-silicate rims around the recrystallized chert nodules as a diffusive mass transfer process between chert and calcite at high activities of CO_2. The equilibrium fluid composition calculated from mineral equilibria for the calc-silicate rim of a nodule at the peak of metamorphism has a minimum X_{CO_2} of 0.6 (Joesten, 1983). Joesten ruled out the possibility of convection of meteoric-hydrothermal H_2O around the pluton during the peak of metamorphism because of the almost magmatic temperatures of the country rocks at the contact and because of the CO_2-rich composition calculated for the fluids. The stable isotopic analyses of this study (below) support his conclusion.

The sampling traverse for this study is about 500 m long, is roughly perpendicular to the contact, and follows a horizon in the limestone that contains chert nodules (see Joesten, 1977). Thin rims of wollastonite observed on the nodules at distances of approximately 105 m from the intrusive contact are the lowest-grade macroscopic evidence of the contact metamorphism. At higher-metamorphic grade, an increasingly complex mineral zonation that includes tilleyite, spurrite, and rankinite replaces the simple wollastonite rim (Fig. 2a; also, see Joesten, 1974; and especially, Joesten and Fisher, 1988, their Fig. 18). Within the chert nodules themselves, the effect of contact metamorphism is mainly an increase in the grain size of quartz toward the contact (Joesten, 1983).

Analytical results

Stable isotope analyses

Preliminary stable isotope analyses show that $\delta^{18}O$ values of quartz in the chert stay constant, essentially at sedimentary values of about 18‰, right up to the contact with the intrusion. Whole-rock $\delta^{18}O$ values of samples of the intrusion are 5.7 ± 0.5‰. If a pervasive fluid flow occurred through the intrusion and aureole during the high-temperature metamorphism, it is most likely that the $\delta^{18}O$ values of quartz in chert (17–18‰) would have been substantially lowered, especially near the contact. C and O isotope ratios of carbonates are shifted only in association with the bleaching seen around the nodules and in the veinlets emanating from the nodule (Fig. 2a). The δ values of carbonates in the bleached and transition zones are much lower than those in the unbleached zone (Fig. 2b). The depletion zone of ^{18}O and ^{13}C in the marble concentrically encloses the nodule. This pattern is complicated where depletion halos of two adjacent nodules overlap, where values as low as 12‰ $\delta^{18}O$ and −0.5‰ $\delta^{13}C$ were measured. The symmetry of the isotopic depletion halo demonstrates that the calc-silicate nodule was the source of the depletion. Baumgartner et al. (1991) attributed these shifts to the wollastonite-forming reactions. They demonstrate on the basis of mass-balance calculations that the overall isotopic shift of the nodules, including host rock, can be attained by a loss of CO_2 alone; an influx of external fluids is not necessary. If CO_2

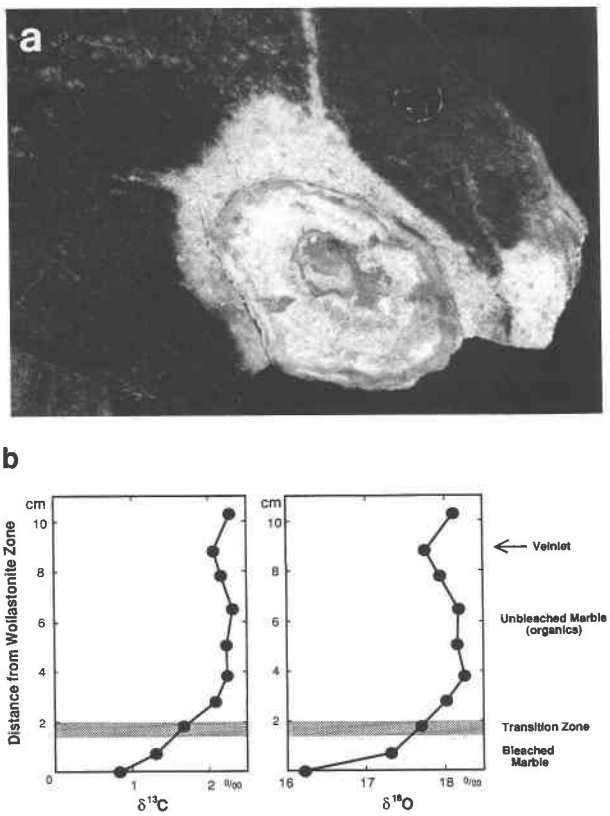

Fig. 2. (**a**) A nodule in sample CR77. The inner core of the recrystallized chert is rimmed by calc-silicate reaction zones composed mainly of wollastonite. The nodule in turn is rimmed by a zone of marble, which appears bleached because of the loss of organic material present in the unbleached marble farther out. Note the veinlet of bleached marble emanating from the nodule. The sample was collected at ~60 m from the intrusive contact. A penny for scale. (**b**) Stable isotopic values of calcite around the chert nodule in **a** showing the depletions in the bleached zone in the marble and near the veinlet that cuts an unbleached portion of the sample.

produced from calcite breakdown at the calcite-wollastonite boundary partially exchanged with the surrounding calcite before escaping from the rock, the zoning shown in Figure 2b would be produced. Within approximately 20 m of the intrusive contact, a few veinlets of coarse calcite can be found; these are the only macroscopic indicators of possible fluid infiltration.

Fluid-inclusion characteristics

In the core of a nodule at ~70 m from the intrusive contact, small fluid inclusions (<1–3 μm) are fairly uniformly dispersed throughout quartz grains in the metamorphosed chert (Fig. 3). The average grain diameter of quartz is approximately 55 μm. Most of the grains have clear rims of 3–15 μm free of inclusion and a core containing a cloud of inclusions. There is no other type of fluid inclusion in this sample. The 70-m sample (CR80a) is also referred to below as the lower-grade sample.

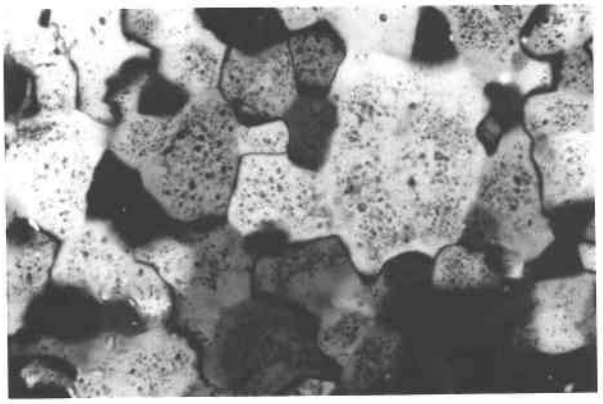

Fig. 3. Fluid inclusions in the lower-grade sample (CR80a). Note the homogeneous distribution of the inclusions and the clear rims along grain boundaries. The scale width of the photo is approximately 330 μm.

At 50 m from the contact, the average grain size of quartz is about 250 μm, and fewer than half of the grains contain a cloud at the core (Fig. 4). Where present, the cloud has a diameter of 20–50 μm (similar to the lower-grade sample) and contains inclusions generally <1–5 μm in length. Many of the clouds are surrounded by larger inclusions with negative crystal shapes, the best example of which is shown in Figure 5a. Other inclusions, not associated with clouds, vary in morphology from negative crystal to irregularly shaped. They occur isolated, in a cluster, or in a healed fracture. The 50-m sample (1021) is also referred to below as the medium-grade sample.

The samples closer to the contact (12, 7, and 2 m; average grain sizes 500, 600, and 1500 μm) contain no quartz grains with inclusion clouds. However, there are other fluid inclusions in the quartz, commonly occurring in clusters and trails. Acicular, solid inclusions up to ~150 μm long (mostly sodium silicon hydrate and wollastonite as determined by electron microprobe analyses) are common along grain boundaries but also extend into the quartz grains. They are obviously retrograde in origin, possibly replacing wollastonite. Some of these solids (sodium calcium silicon hydrate) are associated with fluid inclusions. These samples (1011, CR68, and CR72) are referred to as the highest-grade samples.

Microthermometry and Raman analyses

Microthermometric analyses of the aqueous inclusions in four of the samples were obtained by using a heating-freezing stage (U.S. Geological Survey modified by Fluid, Inc.). Raman analyses were conducted by E. Burke at the Free University, Amsterdam, using a Microdil-28 Raman microspectrometer (Burke and Lustenhouwer, 1988) with a multichannel detector. Chips from the 70- and 50-m samples were also surveyed by J. Reynolds under intense ultraviolet light (365 ± 5 nm). No fluid inclusions were observed to fluoresce, suggesting that concentrations of aromatic hydrocarbons are below the detection level of the method.

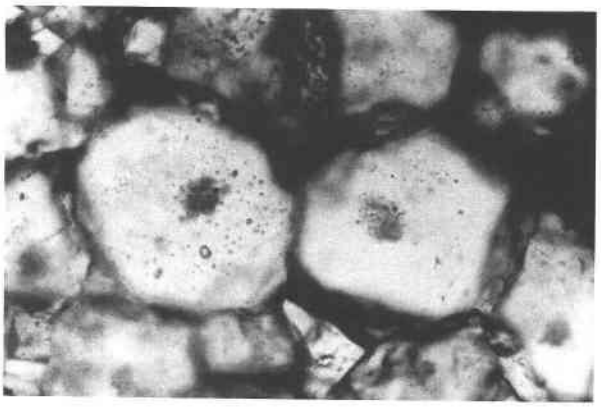

Fig. 4. Fluid inclusions in the medium-grade sample (1021). Note the larger grain size and that clear rims are much wider relative to the diameter than those in the lower-grade sample (Fig. 3). The scale width of the photo is approximately 660 μm.

Most of the inclusions in the 70- and 50-m samples are too small for either microthermometry or individual Raman analysis. A small number of inclusions large enough for observations of phase behavior contain dilute aqueous fluids without an obvious trace of CO_2 or CH_4; no clathrate melting was observed. However, the inclusions are too small (<5 μm) to rule out the presence of carbonic components in these inclusions by microthermometric methods. There is a small, broad CO_2 peak in the Raman spectrum of a cloud in the 50-m sample. Micro-FTIR analysis does reveal the presence of CO_2 and H_2O as discussed below. Melting temperatures (T_m) of ice of measurable inclusions in the clouds are -1.0 to -6.4 °C, corresponding to salinities of 1.7–9.7 equivalent wt% NaCl. Homogenization temperatures (T_h, to the liquid) range from 339 to 395 °C.

Some of the larger inclusions with negative crystal shapes at the periphery of the cloud in the 50-m sample shown in Figures 5a and 5b contain dilute to moderately saline aqueous fluids similar to those in the cloud that could be analyzed (Table 1). Raman analyses show, however, that small amounts of CO_2 and CH_4 are also present in these peripheral aqueous inclusions. Other inclusions at the periphery of the cloud are CO_2 rich and have at most a trace of CH_4, as determined by Raman analyses. Most of the CO_2-rich inclusions probably also contain H_2O: in some, an aqueous phase can be observed in the

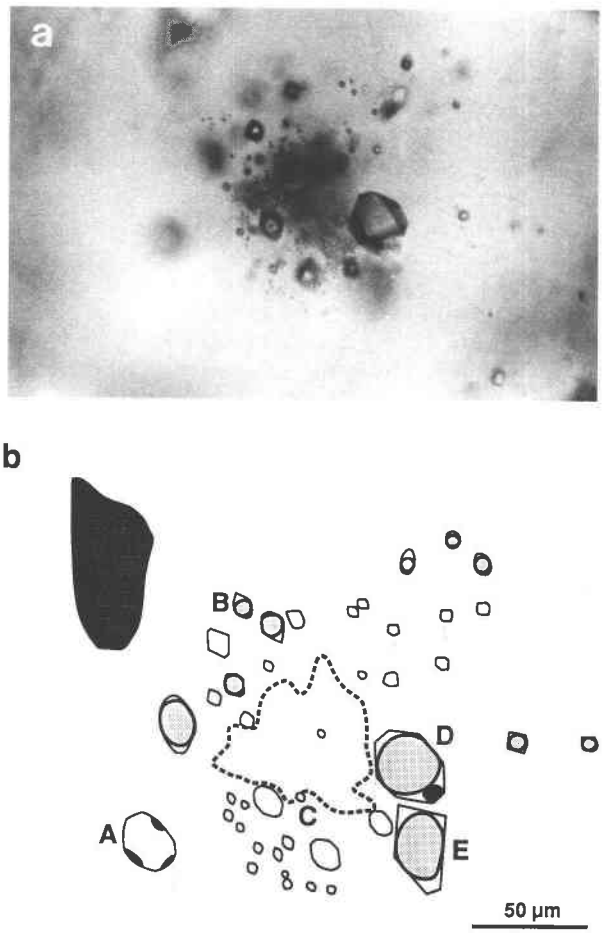

Fig. 5. (**a**) A cloud of fluid inclusions with peripheral larger inclusions with negative crystal shapes in the medium-grade sample (1021). See **b** for scale. (**b**) A sketch of the cluster of inclusions in **a**. White areas = CO_2-rich inclusions; lightly shaded areas = vapor phase in aqueous inclusion; darkly shaded areas = solid phases; dashes = outline of the cloud of inclusions; A–E, see Table 1.

small irregularities in the cavity wall and at the corners of the inclusion cavity. Of the inclusions in the 50-m sample that are not directly associated with a cloud, a majority contain dilute aqueous fluids. The remainder, probably much less than 25%, contain mixed H_2O-CO_2, H_2O-CH_4, and CO_2-CH_4 fluids.

TABLE 1. Results of microthermometric and Raman analyses of inclusions around the cloud in sample 1021, Figures 5a and 5b

Inclusion	T_m ice	T_m carb	T_m cl	No. pRT	No. s	Result of Raman analyses
1021A-b3 A	−7.2	−57.0	8.0	2	0	$CO_2 \gg CH_4$
1021A-b3 B	n.o.	−57.0	n.o.	3	1	$CO_2 \gg CH_4$; solid, not silicate or carbonate, probably salt
1021A-b3 C	−1.7	n.o.	n.o.	2	0	
1021A-b3 D	n.o.	−56.9	n.o.	4	3	
1021A-b3 E	n.o.	n.o.	n.o.	2	0	$CO_2 \gg CH_4$; a small amount of H_2O observed

Note: T_m ice = melting temperature, aqueous phase; T_m carb = melting temperature, carbonic phase; T_m cl = melting temperature, clatherate; no. pRT = number of phases at room temperature; no. s = number of solids; n.o. = not observed.

All inclusions analyzed in the highest-grade samples (1011, CR72) contain aqueous fluids with variable salinity from 0 to 19.7 equivalent wt% NaCl without a trace of carbonic fluids; no clathrate melting was observed. Most homogenize to the liquid phase, but a few homogenize to the vapor phase. Homogenization temperatures (T_h) range from 250 to 460 °C. Pressure-temperature conditions at the peak of metamorphism (>600 °C and ~325 bars) dictate that peak metamorphic inclusions in these rocks containing any common metamorphic fluid (e.g., H_2O, H_2O-NaCl, CO_2 CH_4, N_2, and their mixtures) would have trapped relatively low-density fluid in a one-phase field (vapor). Both T_h and phase behavior of the inclusions that homogenize to the vapor phase are consistent with the inclusions being peak metamorphic. However, these are all aqueous inclusions and do not contain the CO_2-rich fluids predicted from the phase relations of the calc-silicate rim assemblage (Joesten, 1976). The small size of the nodules and the fact that wollastonite is present in the nodules of the medium- to highest-grade samples argues for similar peak metamorphic fluid compositions within the nodule and its calc-silicate rim.

Micro-FTIR analyses

The clouds of inclusions were analyzed using an infrared microscope attached to a Bio-Rad FTS-40 spectrometer. Square apertures of 10–15 μm were used to isolate portions of the clouds for analysis. The spectra from the clouds contain distinct peaks for both H_2O and CO_2 (Fig. 6) and indicate that subequal amounts of the two fluids are present (Brown and Vry, 1990). Comparison of the spectra in Figure 6 from the clouds in the medium- and lower-grade samples indicates that although the relative abundance of H_2O and CO_2 in two samples are somewhat different, both samples contain substantial amounts of H_2O and CO_2. (It is not possible to quantify this difference at present. Optical and geometric effects are still being examined and may eventually lead to a semiquantitative protocol for making these analyses.) Different parts of a cloud in the 70-m sample have different apparent proportions of H_2O to CO_2. Infrared analyses are not able to distinguish a homogeneous group of H_2O-CO_2 inclusions from a mixed group of H_2O and CO_2 inclusions. The variability in amounts of fluids indicated by the differences in spectra could reflect the fact that either such clouds consist of mixed groups of discrete H_2O and CO_2 inclusions in different proportions or that fluid composition varies from cloud to cloud. The variability in fluid composition in turn could reflect the heterogeneities in the material from which the inclusions formed, as discussed below.

Origin of fluid inclusions

The distribution of the inclusions as clouded cores in the quartz grains of the lower-grade sample (Fig. 3) indicates that they are not likely to have trapped a fluid from which quartz precipitated; they are not primary inclusions in the conventional sense of the term. Neither is it likely that these are secondary or pseudosecondary inclusions trapped along fractures. We conclude that these inclusions in clouds contain fluids whose source was internal. It is not likely, however, that these fluids were exsolved directly from quartz. Although chert or its precursor (such as opal CT: e.g., Malieva and Siever, 1989) may contain H_2O in substantial amount, it would not be a direct source of the CO_2. A more likely process for producing these fluids, especially the CO_2 (± CH_4), is the breakdown of organic matter present in the premetamorphic chert. The fluids found in these inclusions are reasonable products of such a breakdown. CO_2 and CH_4 are generated from sedimentary organic matter upon heating (e.g., Rohrback et al., 1984) but the composition of carbonic gas at high temperature (>600 °C) should be CO_2 rich and CH_4 poor (e.g., Shock, 1990, his Fig. 12). Bulk analyses of chert nodules collected well outside the apparent thermal aureole (at approximately 160 and 400 m from the contact) show the presence of H_2O (average = 0.25 wt%), as well as organic C (average = 0.19 wt%). The nodules were analyzed for H_2O by a wet chemical method and for organic C by coulometric analyses, both at X-ray Assay Laboratory of Don Mills, Canada. Furthermore, petrographic examinations by Y. Héroux of the University of Quebec showed fine particles (<1 μm) of organic matter, with estimated high reflectance in a nodule ~150 m from the contact (personal communication, 1991). The analyzed amount of H_2O (0.25 wt%) and organic C (0.19 wt%) would produce ~6 vol% H_2O/CO_2 inclusions at 600 °C and ~300 bars (for the 70-m sample), with the assumption of an unknown source of O for organic C to produce the CO_2. The estimated amount is reasonably comparable to the amount of inclusions present (see Fig. 3).

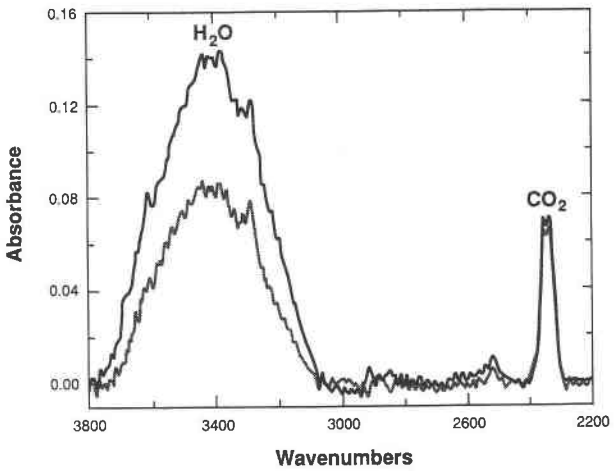

Fig. 6. Micro-FTIR spectra of the inclusion clouds in samples CR80a (heavy line) and 1021 (light line).

Discussion

The following model is proposed to explain the observations made in this study. The complete chronology de-

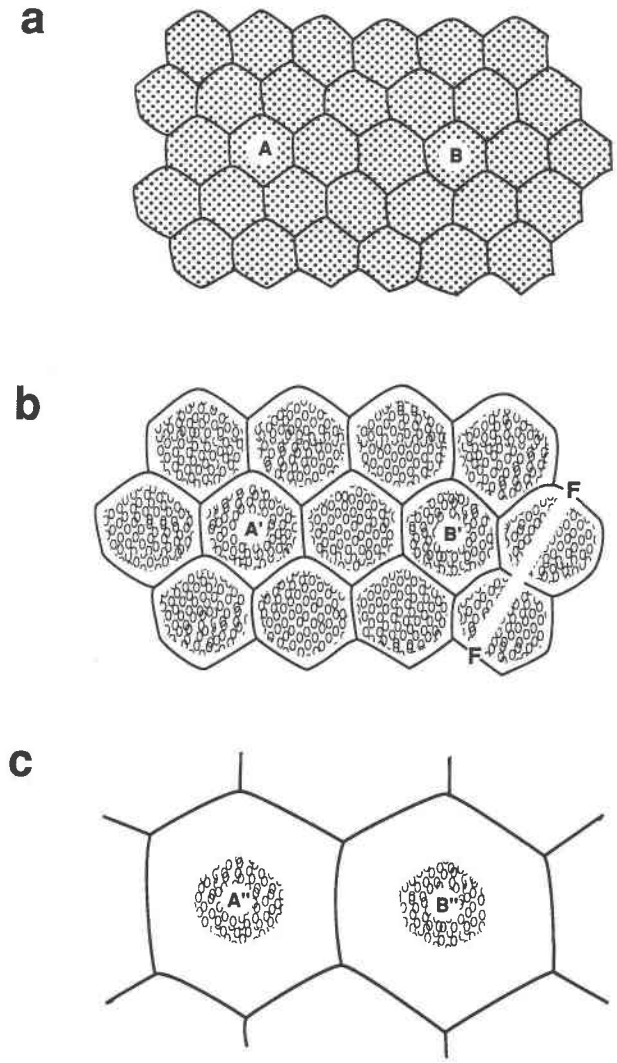

Fig. 7. Cartoon depicting the evolutionary history of fluid-inclusion clouds. (**a**) Upon heating, quartz grains begin to grow and incorporate organic matter present in chert (dots). (**b**) Continued heating causes the thermal breakdown of organic matter. The volatiles liberated are trapped in quartz at the core of the grain as fluid inclusions (small ellipses). F: possible healed fracture. Compare **b** to Figure 3. (**b**, **c**) As quartz grains grow (e.g., A and B to A′ and B′; A′ and B′ to A″ and B″), grain boundaries migrate past inclusions from which fluids are lost, creating the inclusion-free rims. Compare **c** to Figure 4.

scribed would only apply to those samples gathered closest to the intrusion, i.e., those that experienced the full range of temperatures. The samples >70 and 50 m from the contact supply arrested partial histories that provide the evidence to work out the entire story. Briefly summarized, the observations are that bulk analyses of chert at the lowest grade without macroscopic contact effects reveal the presence of both H_2O and organic C. Quartz grains in a metamorphosed chert nodule (with wollastonite reaction rims now retrogressed to calcite) at ~70 m from the intrusive contact contain very small inclusions as a cloud at the core. The cloud occupies 40–85% of the grain in volume. Microthermometry, Raman, and micro-FTIR analyses show that these inclusion clouds contain subequal but variable amounts of H_2O and CO_2. At ~50 m from the contact, the quartz grains have grown approximately five times in diameter from those in the 70-m sample and fewer than half of the grains contain a cloud at the core. The cloud constitutes only 2–3 vol% of the grain at the core. The clouds in the 50-m sample also contain H_2O and CO_2. However, other types of inclusions in more normal modes of occurrence, as solitary inclusions and in clusters and trails, are abundant in the 50-m sample. Most of the inclusions not directly associated with the cloud are aqueous inclusions, with fewer than 25% containing H_2O-CO_2-CH_4 fluids. In the samples taken less than 12 m from the contact, there are no quartz grains with inclusion clouds, but other types of inclusions are abundant, all containing aqueous fluid; carbonic fluid is completely absent. The H_2O/CO_2 ratio of fluid (summed over all inclusions) increases with increasing metamorphic grade.

The quartz nodules now present in the metamorphic aureole must have originally formed as chert or opal and must have contained a small amount of organic matter and H_2O. Initial heating of the limestone and the nodules caused the microcrystalline silica to begin to recrystallize and dehydrate. The organic matter in the rock was, at this point, simply included in the coarsening quartz grains (<50 μm) as solid inclusions (Fig. 7a). Continued heating (at a given point) in the expanding aureole eventually caused the thermal breakdown of the organic matter while the silica host continued to dehydrate. The liberated volatiles (H_2O, CO_2, CH_4) were trapped essentially in situ and now occupy the central 30–50 μm of most of the grains in the fine- to moderately coarse-grained nodules collected >50 m from the contact (Fig. 7b). A few linear inclusion-free zones present in the lower-grade sample represent fractures, now healed, through which some of the early fluids were lost. The likely source of the small amount of salt component present in the aqueous inclusions is sea water trapped in the pores or in marine organic matter. The salt content of quartz in the 70-m sample is estimated from inclusion abundance and salinity of the fluid to be on the order of 0.002 equivalent wt% NaCl or a Cl content of ~0.001 wt%.

The coarsening of some of the quartz grains occurred at the expense of other grains in the nodules (Figs. 7b, 7c). As the quartz dissolved and reprecipitated on the growing grains, the early-generated fluids were lost from the fluid inclusions in the dissolved grains and may have escaped from the rock. The larger inclusions with negative-crystal shapes that surround the cloud in grains from the 50-m sample (Fig. 5) are most likely coalesced early inclusions and may represent the first stage in this remobilization. However, some additional factor, other than surface-energy difference, drove the inclusions in the periphery of the cloud to coalesce while those in the core

did not. One possibility is a mechanical instability exerted by the proximity of grain boundaries.

Samples collected from closer to the contact (<12 m) experienced still higher temperatures and underwent greater degrees of grain coarsening. The inferred complete loss of the early formed core inclusions from the highest-grade rocks cannot be attributed to the grain growth alone because grain boundaries are not likely to have migrated through the cores of growing grains during the coarsening process, as shown in Figure 7. Two processes contributed to the progressive loss of inclusions with increasing metamorphic grade. First, the isochores for the early lower-temperature (and higher-density) inclusions would have steep *PT* slopes, and therefore substantial heating should cause enough pressures in the inclusions for their decrepitation, leading to the loss of fluids from the system. Second, these highest-grade samples have undergone extensive annealing recrystallization at high temperatures that tends to rid quartz of its defects and impurities. This interpretation is not inconsistent with the presence of abundant aqueous inclusions in the higher-grade nodules. These inclusions most likely trapped retrograde fluids that circulated through the inner aureole. Some of these inclusions are clearly associated with retrograde minerals. This conclusion also supports the conclusion of Joesten (1983), which indicated the lack of hydrothermal circulation during peak metamorphism.

The results show that prograde fluids can in some circumstances be preserved as fluid inclusions in contact-metamorphic rocks. Whether this conclusion can be extended to regionally metamorphosed rocks with generally attendant deformation is an important but unanswered question. Vry and Brown (1991) present evidence from the Archean Pikwitonei domain in Manitoba that some contact metamorphic garnets contain early fluid inclusions that have survived subsequent granulite-facies regional metamorphism. Although the Christmas Mountains rocks have not been subject to such dynamic metamorphism, some have been heated to (and beyond) the high temperatures of high-grade regional metamorphism and still preserve prograde inclusions. Thus the possibility that prograde inclusions may survive should be considered for some metamorphic inclusions, especially those that appear texturally to be early but do not have the composition predicted for peak metamorphic fluids.

Acknowledgments

We gratefully acknowledge the contributions of the following people and organizations to this study. E. Burke of the Free University, Amsterdam, performed analyses by the Raman probe, supported by the Netherlands Organization for Scientific Research. Douglas Rumble provided access to his carbonate stable isotope line at the Geophysical Laboratory. Silicate stable isotope analyses were performed by Kevin Baker in the laboratory of John Valley, University of Wisconsin, Madison. Y. Héroux provided petrographic identification of organic matter. Jim Reynolds surveyed the samples for fluorescence under ultraviolet light. George Fisher provided some of the samples. The paper has been greatly improved by critical and helpful reviews by M.L. Crawford, James O'Neil, R. Burruss, and L.S. Hollister. We especially thank Ray Joesten for encouragement and helpful discussions. T.B. Henderson, D. Smith, and the First City Asset Servicing Company generously granted access to their properties. The study has been supported by NSF grants 8917185 to S.N.O., 9106313 to L.P.B., and 8805470 and 8805289 to P.E.B.

References cited

Baumgartner, L.P., Valley, J.W., and Olsen, S.N. (1991) Extreme isotopic zonation around chert nodules from a contact aureole, Christmas Mountains, Texas. Geological Society of America Abstracts with Programs, 23, A50.

Brown, P.E., and Vry, J.K. (1990) Applications of micro-FTIR spectroscopy to fluid inclusions. PACROFI III, 3, 23–24.

Burke, E.A.J., and Lustenhouwer, W.J. (1988) The application of a multichannel laser Raman microprobe (Microdil-28) to the analysis of fluid inclusions. Chemical Geology, 61, 11–17.

Crawford, M.L., and Hollister, L.S. (1986) Metamorphic fluids: The evidence from fluid inclusions. In J.V. Walther and B.J. Wood, Eds., Fluid-rock interactions during metamorphism. p. 1–35. Springer-Verlag, New York.

Ferry, J.M., and Burt, D.M. (1982) Characterization of metamorphic fluid composition through mineral equilibria. In Mineralogical Society of America Reviews in Mineralogy, 10, 207–262.

Hollister, L.S. (1990) Enrichment of CO_2 in fluid inclusions in quartz by removal of H_2O during crystal-plastic deformation. Journal of Structural Geology, 12, 895–901.

Joesten, R. (1974) Local equilibrium and metasomatic growth of layered calc-silicate nodules from a contact aureole, Christmas Mountains, Big Bend region, Texas. American Journal of Science, 274, 876–901.

——— (1976) High-temperature contact metamorphism of carbonate rocks in a shallow crustal environment, Christmas Mountains, Big Bend region, Texas. American Mineralogist, 61, 776–781.

——— (1977) Mineralogical and chemical evolution of contaminated igneous rocks at a gabbro-limestone contact, Christmas Mountains, Big Bend region, Texas. Geological Society of America Bulletin, 88, 1515–1529.

——— (1983) Grain growth and grain-boundary diffusion in quartz from the Christmas Mountains (Texas) contact aureole. American Journal of Science, 283-A, 233–254.

Joesten, R., and Fisher, G. (1988) Kinetics of diffusion-controlled mineral growth in the Christmas Mountains (Texas) contact aureole. Geological Society of America Bulletin, 100, 714–732.

Malieva, R.G., and Siever, R. (1989) Nodular chert formation in carbonate rocks. Journal of Geology, 97, 421–433.

Mullis, J. (1987) Fluid inclusion studies during very low-grade metamorphism. In M. Frey, Ed., Low temperature metamorphism, p. 162. Blackie, New York.

Roedder, E. (1984) Fluid inclusions. Mineralogical Society of America Reviews in Mineralogy, 12, 644 p.

Rohrback, B.G., Peters, K.E., and Kaplan, I.R. (1984) Geochemistry of artificially heated humic and sapropelic sediments—II: Oil and gas generation. American Association of Petroleum Geologists Bulletin, 68, 961–970.

Shock, E. (1990) Geochemical constraints on the origin of organic compounds in hydrothermal systems. Origin of Life and Evolution of the Biosphere, 20, 331–367.

Spear, F.S., and Selverstone, J. (1983) Water exsolution from quartz: Implications for the generation of retrograde metamorphic fluids. Geology, 11, 82–85.

Sterner, S.M., Hall, D.L., and Bodnar, R.J. (1988) Synthetic fluid inclusions. V. Solubility relations in the system NaCl-KCl-H_2O under vapor-saturated conditions. Geochimica et Cosmochimica Acta, 52, 989–1005.

Vry, J.K., and Brown, P.E. (1991) Texturally-early fluid inclusions in garnets: Evidence of the prograde metamorphic path? Contributions to Mineralogy and Petrology, 108, 271–282.

Manuscript received October 11, 1991
Manuscript accepted April 28, 1992